INTERNATIONAL JOURNAL OF INTEGRATED ENGINEERING
ISSN: 2229-838X e-ISSN: 2600-7916

IJIE

Vol. 17 No. 8 (2025) 169-180
https://publisher.uthm.edu.my/ojs/index.php/ijie

TiungLap: A Quadcopter Drone for Window Cleaning with an Integrated Pressure Washer Tethering System

Ahmad Fathan Fadzulli[1], Omar Mohd Faizan Marwah[2]*, Mohammad Zulafif Rahim[3], Siti Juita Mastura Salleh[3], Zamri Omar[1], Suhaimi Hassan[1], Reazul Haq Abdul Haq[1]

1 *C-Drone Research Centre, Faculty of Mechanical Engineering and Manufacturing, Universiti Tun Hussein Onn Malaysia, Parit Raja, 84600, MALAYSIA*
2 *Research Centre for Unmanned Vehicle, Faculty of Mechanical Engineering and Manufacturing, Universiti Tun Hussein Onn Malaysia, Parit Raja, 84600, MALAYSIA*
3 *Avitex Solution (M) Sdn. Bhd., Faculty of Mechanical Engineering and Manufacturing, Universiti Tun Hussein Onn Malaysia, Parit Raja, 84600, MALAYSIA*

*Corresponding Author: mdfaizan@uthm.edu.my
DOI: https://doi.org/10.30880/ijie.2025.17.08.016

Article Info

Received: 5 May 2025
Accepted: 30 November 2025
Available online: 31 December 2025

Keywords

UAV, window cleaning, high-rise building, thrust analysis, power analysis, PID tuning

Abstract

The TiungLap drone, developed to address the high risks and inefficiencies associated with traditional high-rise window cleaning, integrates a tethered high-pressure washer system to improve safety and operational time. The drone features advanced GPS navigation, real-time monitoring, and LiDAR-based obstacle avoidance for precise cleaning in complex environments. The objective of this study was to optimize the thrust, power consumption, and control stability of the drone during cleaning operations. Utilizing four X9 motors, the drone achieved a maximum thrust of 21.23 kgf per motor, ensuring sufficient lift to handle its 22 kg payload. Power analysis revealed the motors consumed 4790.2W each, contributing to a total system power consumption of 7421.25W. A key challenge was stabilizing the drone under the influence of external forces from the tethered hose, which was addressed through manual tuning of the PID controller. This tuning reduced roll error by 94.9% and pitch error by 87.8%, significantly improving drone stability. Future research should focus on enhancing flight endurance and further optimizing control algorithms to handle external forces more effectively.

1. Introduction

With the relentless progress of modern technology, researchers are increasingly focused on exploring innovative solutions to either replace human labor or enhance human tasks while minimizing associated risks [1]. Among these advancements, the application of technology to high-risk activities, such as cleaning windows on towering skyscrapers, not only mitigates potential harm to human workers but also streamlines the task's efficiency [2].

The traditional techniques to maintain these glass structures are not only time consuming and costly but also endanger the lives of workers responsible for maintaining them. For instance, Merdeka 118 is a 118-storey, 678.9m -tall mega skyscraper in Kuala Lumpur, Malaysia that require a team of window cleaners from VerticalPro Sdn. Bhd. labor to ensure the building's pristine appearance [3].

1.1 Window Cleaning: Modern vs Traditional Method

Advancements in autonomous technology have led to the development of various solutions for efficiently and safely cleaning windows of high-rise buildings. A significant milestone in window cleaning robots is the introduction of the first commercialization known as WINDORO [4]. Other notable robots in the market include Winbot by Ecovas and Artdog S8 by HUTT [6][7]. These robots are designed lightweight and compact, which aids in their movement across windows and helps in cost reduction. Unfortunately, these models are typically more suitable for household use rather than high building window cleaning. However, Safe Building Cleaning Robot like K3 and J1 by X-Human are small, wall embedded and come with a substantial price tag [7]. The technology regarding window-cleaning robots is continually advancing to address the limitations of current solutions.

A glass curtain wall cleaning robot, equipped with 4 propellers, used to clean window frames with surface groove heights of less than 4cm. It navigates by flexing its roller brush and two scrapers for cleaning method. However, if the surface frame's height surpasses 4cm, the propellers produce a force that pushes the robot away from the wall until it clears the groove height, enabling it to resume its movement along tracked line[8]. Taking advantage of the robot's simple and practical design, alternative solutions employed tracked locomotion mechanisms [2]. GEKKO by SERBOT implements a pair of flat tracks to surmount obstacles measuring 4cm in height and can obtain a cleaning speed of 400 m^2/h [9]. Despite that, this approach results in slower motion and reduced turning ability, thereby decreasing its overall flexibility in multi-axis movement

The drone innovation aims to identify the optimal parameters for the cleaning operation using the UTHM cleaning drone, integrating a high-pressure spraying mechanism into the drone for effective high-rise building cleaning tasks, and evaluating the performance of the spraying system to ensure it achieves satisfactory cleanliness levels during these operations. Unmanned Aerial Vehicles (UAVs) are frequently utilized for non-contact tasks such as surveillance, reconnaissance, and hazard exploration. UAV is common for applications like automated window cleaning, where the drones operate using Radio Frequency (RF) signals to clean glass surfaces[10]. The cleaning mode activates when the drone contacts the window, and the drone's motion is controlled by RF signals [11].

However, releasing the cleaning mechanism destabilizes the system due to altered drone's inertial dynamics. Suction cups for drone adhesion onto glass surfaces are used to mitigate this positional constraint. Meanwhile in power line cleaning, UAV implements an insulator detection and tracking algorithm to control its operations [12][13]. Plus, an autonomous system is used for drone landing on a charging pad also enables the refilling of the cleaning tank to cover larger cleaning areas [14]. While using UAVs for cleaning tasks is beneficial, a significant drawback is their limited endurance and short operational time, which reduces cleaning efficiency. With tethered spraying systems will resolve the main challenges discussed in previous work including stability and speed of motion, cleaning performance and flight endurance.

2. Drone Ecosystem Setup

2.1 Drone Feature

After conducting thorough research on contemporary skyscrapers window cleaning robots and drones, TiungLap distinguishes itself through 3 features including a tethered cleaning and powering system, real-time monitoring capabilities, and the utilization of robust cleaning equipment.

The tethered design of TiungLap in Fig. 1 focuses on leveraging the Karcher High-pressure washer HDS 6/14 C to supply heated solutions, either water or cleaning solution, and pressure up to 120 Bar [15]. This system not only enhances cleaning efficiency but also eliminates the need for onboard tanks, thus reducing the drone's weight. The drone employs a hybrid power system, utilizing LiPo battery and DC generator from the EV under carriage, allowing for prolonged cleaning operations and increased flight endurance until the DC generator cut off. This setup mitigates potential safety risks associated with cable entanglement during the drone's cleaning operations while maintaining optimal performance due to flexibility of pressurized hose.

Real-time monitoring is a key feature in TiungLap, facilitating the effective supervision of the drone's cleaning process by the operator. The drone will be controlled remotely using RF through software-controlled instructions in their embedded systems, working alongside onboard sensors and Global Positioning System (GPS). This allows for comprehensive remote control of the drone ensuring safety of the operator and efficient execution of window cleaning tasks.

Int. Journal of Integrated Engineering Vol. 17 No. 8 (2025) p. 169-180

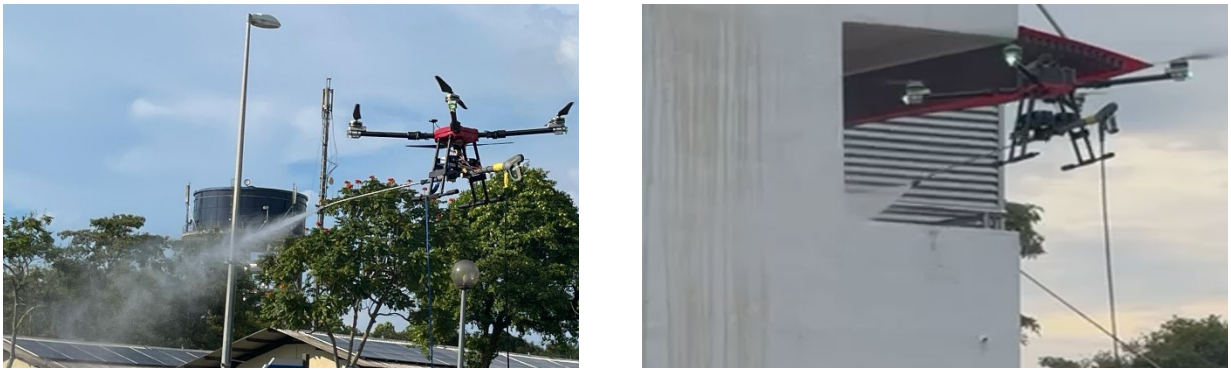

(a) **(b)**

Fig. 1 *Tethered pressurised hose (a) solar panel cleaning; and (b) facade building cleaning*

The primary task of TiungLap is to ensure thorough cleaning of skyscraper windows. Therefore, the drone is equipped with specialized cleaning materials and tools that meet safety, weight distribution, power system, and stability constraints. TiungLap employs a grounded pressure washer with an onboard spraying wand, allowing the drone motors to exert only necessary thrust and pressure to remove dirt from windows while maintaining a safe distance from water splashes which will affect electronic circuits. The pressure washer's adjustable pressures and temperatures offer versatile cleaning power for different high-rise building structures due to head loss. Additionally, TiungLap integrates a LiDAR system for obstacle avoidance to ensure safe distances and optimal distance for enhancement of cleaning performance.

2.2 Drone Architecture

The TiungLap drone is designed for efficient cleaning of skyscraper windows, with various onboard components working together as in Fig. 2. The Flight Controller (FC) acts as the central processor, managing all components based on commands from the Remote Controller (RC). The obstacle avoidance system is critical for the safe operation of the TiungLap drone. It utilizes an omnidirectional LiDAR sensor to scan the environment and detect obstacles in real time. This information is fed into the flight controller, enabling the drone to navigate around obstacles and maintain a safe distance from the building surface[4]. This capability is vital for preventing collisions and ensuring the drone's stability during cleaning operations.

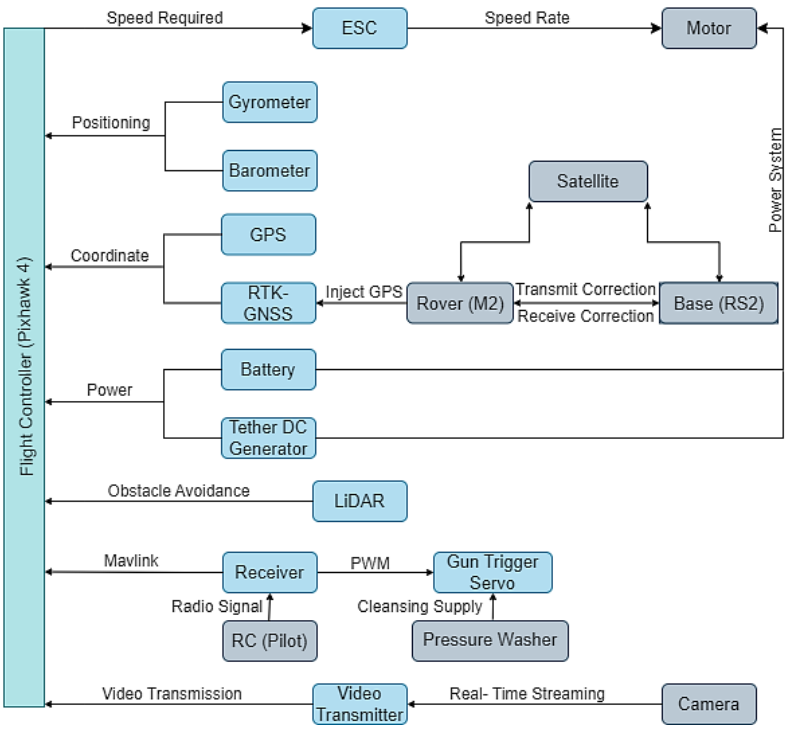

Fig. 2 *TiungLap architectural block diagram*

The TiungLap drone's cleaning system includes a ground pressure washer and a gun trigger servo. The pressure washer supplies the necessary cleaning solution and pressure to remove dirt and grime from building windows. The gun trigger servo controls the activation and flow of the cleaning solution based on commands received from the FC. This setup allows the drone to apply the appropriate amount of cleaning force, ensuring effective cleaning without damaging the windows or the drone.

For precise navigation, the TiungLap drone relies on a GPS and RTK-GNSS provides basic global positioning data within meter, while RTK-GNSS significantly enhances this accuracy within centimeter [5]. The RTK-GNSS setup includes a Rover-Drone that injects corrected GPS count into the FC, and a Base station that communicates with satellites to receive correction data. This ensures that the GPS data collected by the drone is highly accurate, enabling precise positioning and navigation during proximity cleaning tasks. The TiungLap drone is equipped with a video transmission system for real-time monitoring of the cleaning operations. The camera will capture live footage, which is sent to the ground station, allowing operators to oversee and adjust the process as needed. This system ensures thorough cleaning, precise positioning, and safe operation.

2.3 Onboard Integration Setup

Onboard Component: Pixhawk 4 is used as the Flight Controller to control signal throughout the system. X9 Motor is used to create a thrust of 21Kgf each which consists of 4 motors controlled by each arm's 150A Electronic Speed Controller (ESC).X9 Motor is built in with its own ESC and connected to PDB HolyBro PM07. From the PDB the 2 outsource Power 1 and Power 2 wire will supply power to Pixhawk 4. The FMU and I/O PWM cable will transfer data to control all X9 motors.

Structural Chassis: TiungLap is implement using a quadcopter drone with a large carrying capacity up to 22 Kg[6]. All 4 arms and framework are made from carbon fiber that makes it a very lightweight option with high structural stability and strength [17][18].

Remote Controlling System: ELRS is connected via GPS RX-TX in Pixhawk 4 Port. ELRS is renowned for its long-range capabilities, allowing to control of TiungLap over 2Km distances using 25mW HappyModel EP2 [9] which reliable for window cleaning accessibility since the highest skyscraper only. 828m (2717 ft) [10]. Meanwhile, the transmitter from RadioMaster TX12 helps to control multiple servos output up to 16 channel availability.

Global Positioning **System**: In RTK-GNSS System, satellite facilitates communication between the Base station (Emlid RS2) and Rover-Drone (Emlid M2), allowing the Base station to receive correction data from the satellites and transmit it to the Rover-Drone [21][22].For Primary GPS, TiungLap equipped with Here3 GPS which is connected to CAN1 while Emlid M2 at TELEM2 port.

Obstacle Avoidance **System**: The detection from the omnidirectional lidar assists the TiungLap operates in proximity high building distancing [12]. As mentioned in Fig. 3, RPLidar A2 is chosen due to the minimum distance as near as 5 cm and as further as 40m range of detection [13]. RPLidar A2 is connected via pin UART i2c to utilize the RX-TX communication protocol.

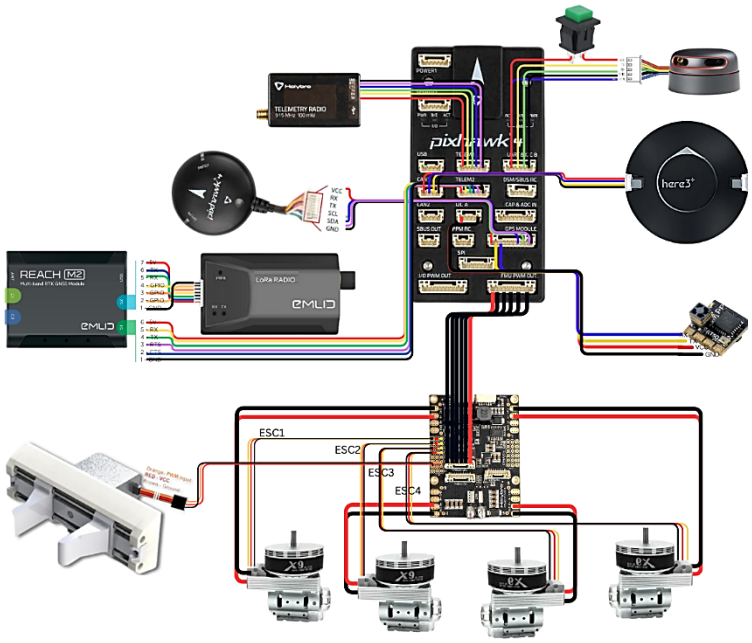

Fig. 3 *TiungLap electrical diagram assembly*

Int. Journal of Integrated Engineering Vol. 17 No. 8 (2025) p. 169-180

2.4 Grounded Integration Setup

2.4.1 Solution Supply system

The drone consumes 240L/Hr at 30 Bar and 560L/Hr at 120 Bar depending on what type of dirt and surrounding building that deal which purposedly design to supply infinite power and unlimited water supply to shorten high rise building cleaning task. Since TiungLap is developed within the area of UTHM, the targeted building of Tunku Tun Aminah Library is covered with glass material which can endure up to 7 GPa[28][29]. The ideal pressure ranging for dirt cleaning is from 50kPa up to 2 Bar [30][31] and temperature of 40°C to 80°C [32][33] which tally with the Karcher HDS pressure washer specifications

2.4.2 Power Supply system

Power Supply System used to maintain full portability of the drone, the battery Herewin 22,000 mAh, 2.74 Kg LiPo is deployed on TiungLap[20]. The battery capacity is what mainly decides the flight time, nevertheless, the higher that battery capacity the more the weight. This cell would last TiungLap 15-20 operational minutes. TiungLap drone is powered with a pair of 6S LiPo battery which a total rated of 44.4 – 50.4V [21] voltage supplied throughout the drone by distributing via HolyBro PM07.

Power consumption will provide insight into the endurance of the drone, and the power required to perform effective cleaning processes. TiungLap has 2 packs of batteries powering the entire system. Both are crucial for supplying the onboard while DC-DC Buck Converter used to power Karcher HDS 6/12. Power consumption of TiungLap were calculated using the simple power equation as follows, where P is power consumed (W), I is current flowing in the component(A), and V is potential difference of the component in(V). The hovering power consumed by each component is shown in Equation 1.

$$P = I \times V \tag{1}$$

Uninterruptible Power Supply (UPS) carriage supplies a continuous voltage of 50.4V from the DC-DC buck Converter modified beneath the carriage cart. Thus, there is no need to land UAV for battery replacement which can increase operational time[22].

3. Methodology

3.1 Flight Tuning Setup

The tensioner should be kept the cable tighten enough for safety purpose to stabilize the drone without overly restricting its movement as Fig. 4. During initial adjustments, we start with a low altitude to ensure safety. When oscillations start, we avoid making large or sudden stick inputs. Reduce the throttle smoothly to land the aircraft while using very slow and small roll and pitch inputs to control the aircraft position.

Value of Derivative (D) Term is used to smooth out the drone's response, reducing overshoot and quick corrections. Increasing (D) value helps dampen oscillations caused by the (P) adjustment. However, excessive (D) can result in sluggish drone movements. Proportional (P) Term gradual increases will enhance the drone's reaction to positional errors. The (P) was increased until the drone begins to oscillate or "bounce" as it corrects itself to slowly fine the optimal reduced value. Integral (I) Term is adjusted to correct any long-term drift or steady-state errors. Increasing the (I) value gradually ensures the drone maintains its position over time. Proportional value is directly proportional to Integral value. When, I value too high can cause the drone to oscillate slowly back and forth[23].

In Mission Planner, perform manual tuning useful to ensure aircraft is stable and confirm that ATC_THR_MIX_MAN and MOT_THST_HOVER are set correctly before flying. If the aircraft already shows oscillations, reduce the (P), (D), and (I) term by 50% until stability is regained. Start by increasing the (D) term in 50% steps until oscillations occur, then reduce it in 10% steps until the oscillation stops. Finally, lower the (D) term by an additional 25%. Next, follow the same process with the (P) term: increase it by 50% increments until oscillation occurs, then reduce it in 10% steps until it stabilizes. Afterward, reduce the P term by a further 25%. Once you adjust the P term, set the (I) term to match the P term

After tuning each component, fine-tuning the PID values crucial to improve flight performance and maintain stability as the drone handles the exerted forces[24]. TiungLap is tested at different altitudes and positions to ensure it behaves consistently in all situations[25]. Testing with the pressurized hose connected simulates various load conditions, revealing how the current PID settings perform under different pressures and directions.

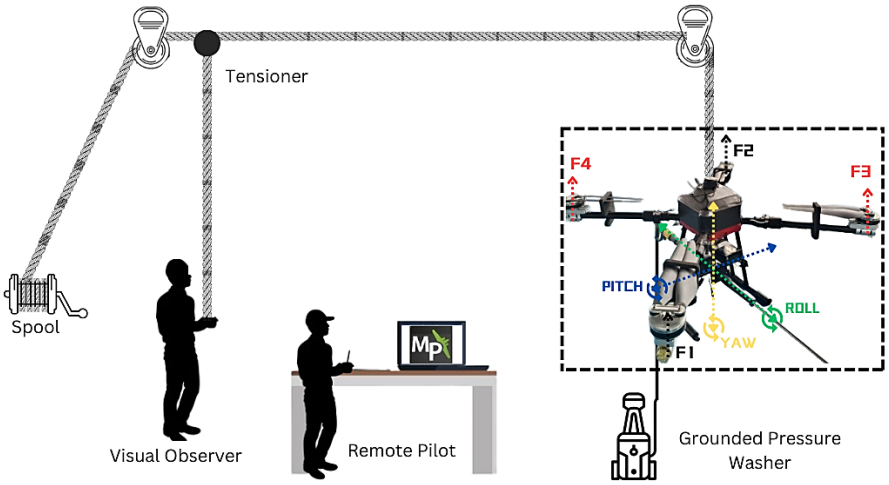

Fig. 4 *Drone flight testing rig*

3.2 Motor Thrust Simulation

When simulating the Hobbywing X9 motor's performance using Scorpion Calc, the motor's specific characteristics from its datasheet come into play, helping to create an accurate model of how it will function in a drone setup. The Hobbywing X9 is a high-performance motor typically used for heavy-lift drones. Some key features of the X9 motor include its KV rating of 110KV, which indicates that for every volt supplied, the motor will spin at 110 RPM under no load. This high KV value means the motor is optimized for quick rotational speeds, making it suitable for larger propellers, which the X9 is often paired with. The motor has a no-load current (Io) of around 2.3A, which is the current the motor consumes when it spins without any load. The motor resistance (Rm) is typically around 0.031 ohms, a value that reflects the internal resistance of the winding and affects both efficiency and heat generation. The weight of the X9 motor is approximately 1400g, a substantial weight that contributes to a lower power-to-weight ratio but provides the torque needed for lifting heavier loads.

In Scorpion Calc layout as Fig. 5, once these values are input, the tool calculates the motor's performance under different conditions. For instance, with a 46V LiPo battery (12S), the motor's power consumption and thrust production can be simulated. With X9's maximum peak current of 150A from its ESC, the motor can draw significant power, efficiently converting much of it into thrust. By pairing the X9 with a 34.7'' diameter with 11" pitch propeller a strong thrust generation is expected. The 2-bladed propeller setup complements the motor's high-torque capability, allowing the drone to carry heavy loads while maintaining stable flight. Additionally, the software evaluates power loss due to heat and inefficiencies. For instance, in Fig. 5, a value of 1.341W/g for dissipated power indicates some energy loss, a factor that needs to be managed during operation.

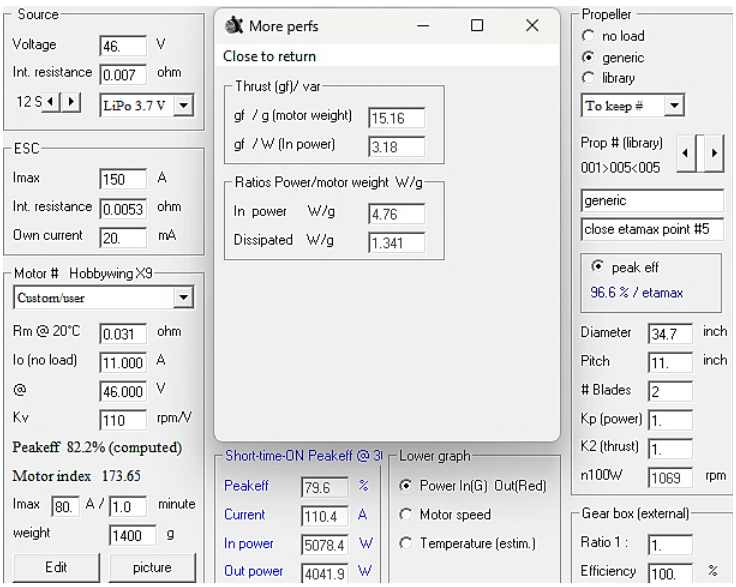

Fig. 5 *Scorpion calc parameter layout*

Int. Journal of Integrated Engineering Vol. 17 No. 8 (2025) p. 169-180

4. Performance Analysis

4.1 Power Analysis

TiungLap has a Maximum Take Off Mass (MTOM) of 22 kg which is supported by 4 motors [6]. Based on Table 1, the drone's theoretical weight is 13,658.5g which is well within half the thrust from the 110kV X9 motor datasheet. Table 1 includes an analysis of both external and onboard systems that exclude the pressure washer as part of the payload. The drone can lift to 20 kg of payload, which is more than enough to handle its total weight ensuring it to not stall.

Table 1 outlines the power consumption of various components in the TiungLap system, split between onboard drone components and grounded equipment. Key onboard elements like the drone chassis and spray lance does not consume power directly, but their weight affects overall power requirements. The X9 motors are the largest power consumers onboard, using 4790.4 W due to the energy needed for flight and maneuvre as motors are generally power-intensive. Other components, like the GPS and flight controller, consume minimal power as they only handle signal and control tasks.

Table 1 *TiungLap component idling power consumptions*

Component	Weight (g)	Classification	Power (W)
Drone Chassis	6000.0	Onboard Setup	NA
Karcher 2m Spray Lance	1400.0		NA
X9motor 110kv [18][37]	5800.0		4790.4
GPS Here3	48.8		0.800
Pixhawk 4	49.0		0.049
RPLidar A2	190.0		3.000
Telemetry HolyBro Sik	22.7		0.500
Mg995 Servo	77.0		7.500
Emlid M2	35.0		1.500
Lora Radio	35.0		1.000
TOTAL TAKE OFF WEIGHT	13657.5	TOTAL TAKE OFF POWER	4804.749
Karcher HDS 6/12c	115600.0	Grounded Setup	3000.000
TOTAL SETUP WEIGHT	142,915.00	TOTAL POWER	7421.249

Moderate power-consuming components include GPS Module that needs 2.3W to scan satellite correction for precision positioning and LoRa radio which requires 1W for long-range communication. Servos and the RPLidar A2 consume more energy due to their mechanical functions and torque requirements due to spinning mechanism. The total take-off power for all onboard components is around 4804.75 W indicate that motors and mechanical component drive the bulk of energy use for the airborne setup.

For grounded components, the Karcher HDS 6/12C, a heavy-duty machine weighing 115.6kg consumes 3kW contributing significantly to total system power. The total power for the entire system, combining both airborne and grounded components, is 7421.249 W. The high-power consumption stems primarily from motors, mechanical parts like servos, and the weight of onboard and grounded equipment, which demand more energy to function effectively.

4.2 Thrust Analysis

The theoretical performance analysis was simulated with Scorpion Calc to measure the motor performance benchmarking. The X9 motor achieved a torque of 11.63 Nm of torque with a 34-inch polymer propeller indicating rotational force required to keep the propeller spinning under load. The output power from Scorpion Calc show 4790.2W for each motor which as average as X9 motor datasheet stated in Table 1 which 4790W. Scorpion Calc determines the efficiency of the motor-propeller combination by calculating the thrust produced, which in this case is approximately 3.18 grams per watt of input power.

The motor speed at Wide Open Throttle (WOT) is 3933 RPM as shown in Fig. 6. This speed indicates speed the motor shaft is rotating when operating at maximum throttle. Since the propeller is directly connected to the motor, it spins at the same speed. This synchronized rotation ensures that the propeller delivers consistent performance. Pitch speed was simulated at 18.3 m/s using the propeller's pitch and rotational speed.

Determination of the potential maximum speed of an aircraft is a crucial factor before flying. A higher pitch speed usually indicates better performance in forward flight but may require more power.

Static thrust is the force generated by the propeller when the aircraft is not moving. In this case, the static thrust is 21.23 kgf whereby each motor theoretically can lift up to 21Kg equivalent to 208.195N. The motor operates with an efficiency of 81.4%, meaning that 81.4% of the electrical power is converted into mechanical power to drive the propeller. The input power to the motor is 6,458 watts, but only 4.159.5 kW are used for propulsion, with the rest lost as heat and other inefficiencies. This efficiency is crucial for determining how effectively the motor uses energy, impacting the flight time and performance.

Fig. 7 shows the performance of Hobbywing X9 110kV motor, focusing on its efficiency (Eta%) and relative RPM as current increases. The red curves represent motor's efficiency at elevated temperature while black curves show motor efficiency at ambient temperatures (30°C) and purple dotted line shows the relative RPM.

Both efficiency curves peak around 80% at 100-150A, with the ambient temperature curve slightly higher. As the current increases, the motor's efficiency rises quickly at first, reaching a peak before gradually declining. At plotted circle, the efficiency is 75.5% when accounting for temperature rise as shown in Fig. 10. This means that the with 34" propeller on X9 motor operates most efficiently at 144.94A current. After this point, efficiency drops because more of the electrical power is lost as heat and other inefficiencies.

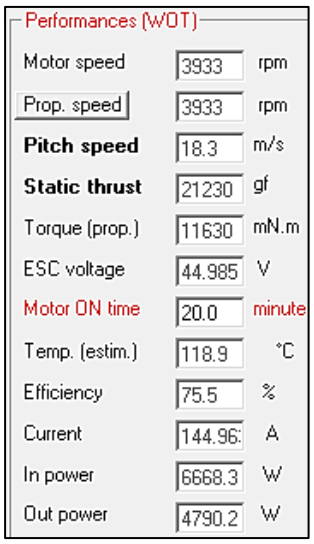

Fig. 6 *WOT X9 motor performance analysis*

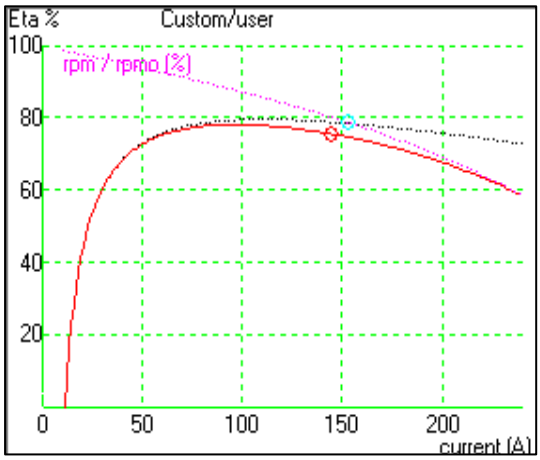

Fig. 7 *Efficiency (η) vs. current (A)*

Fig. 8 *Output power (kW) vs. current (A)*

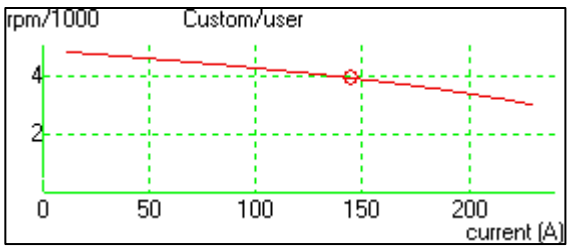

Fig. 9 *RPM vs. current (A)*

Fig. 10 *Temperature (°C) vs. current (A)*

Fig. 7 shows that the small circle on this graph indicates the actual power output at the current level the motor experiences when the 34" propeller is attached. The red trend indicates the output power for arise temperature and the green represent output power at ambient temperature. More electrical power is converted into mechanical power as more current is supplied to the motor.

Int. Journal of Integrated Engineering Vol. 17 No. 8 (2025) p. 169-180

Based on the Fig. 8 trend, output power of the motor increases steadily as the current increases. Since Power Input at particular current is 6668.3 and output power is 4790.2W, the power losses during WOT is 28.16%.

As the current increases, the motor's rotational speed (RPM) decreases. This happens because higher current indicates a higher load, which causes the motor to slow down. Fig. 9 small circle represents the maximum motor's speed under 144.94A current drawn.

The motor's temperature rises as the current increases. This is because more current leads to more heat generation due to power losses within the motor. The small circle on the graph marks the temperature of the motor at the operating current level with the propeller attached, highlighting the importance of managing heat at higher currents.

Fig. 10 illustrates important trade-offs in motor performance. As current increases, efficiency initially rises but then begins to fall, especially at higher temperatures. This highlights ESC needs an effective cooling, particularly when operating at higher currents. Meanwhile, the relative RPM gradually decreases as current increases, showing the motor's speed drops under heavier loads. Overall, this data helps in finding the optimal operating point that balances power output with efficiency and heat management.

4.3 Thrust Analysis

For all P, I and D terms, method of adjustment was the same as shown in Table 2. First, Increase PID value in steps of 50% until oscillation is observed. The value reduces gradually in steps of 10% until the oscillation disappears and finally reduce the by a further 25% for slight adjustments.

Table 2 *PID manual tuning*

	Roll			Pitch			Yaw		
	P	I	D	P	I	D	P	I	D
Initial	0.135	0.135	0.00237	0.135	0.135	0.00360	0.18	0.018	Default
Final	0.069	0.069	0.00243	0.062	0.062	0.00369	0.18	0.018	Default

In Fig. 11 and Fig. 12, show the comparison of pitch and roll for TiungLap before and after tuning. The drone's behavior appears to oscillate, due to the influence of attached pressurized hose. Logically, flow-induced forces from flexible hose can destabilize a quadrotor during fluid ejection, necessitating a combined feedforward-feedback control strategy that can improve stability by over 61%[27]. The hose causes external forces and constraints, making the drone harder to maintain stability and match its desired roll accurately, especially in dynamic flight condition[24][28].

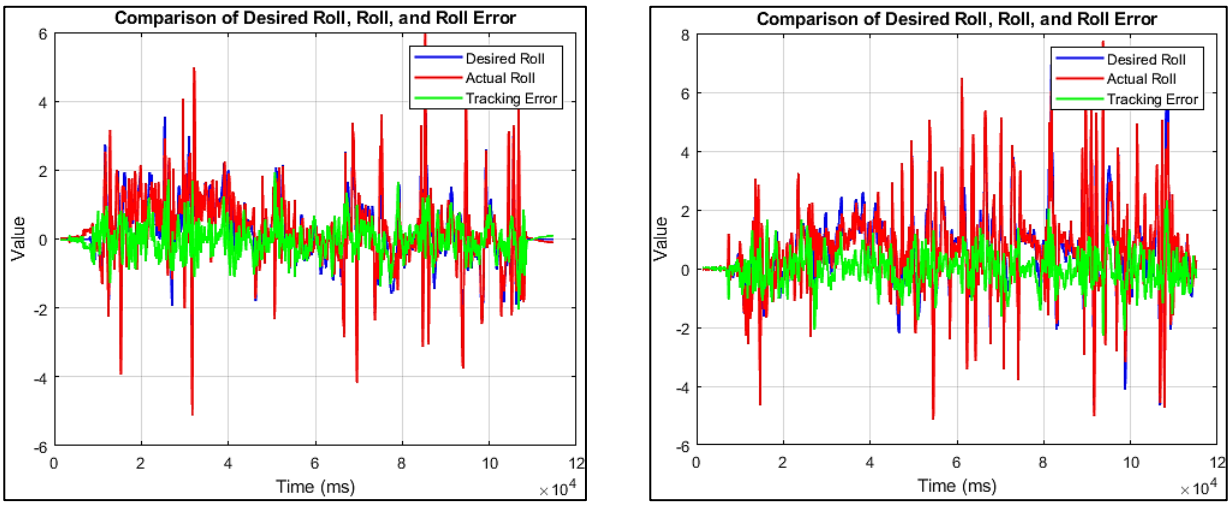

(a) **(b)**

Fig. 11 *(a) Roll vs desired roll before tuning & (b) Roll vs desired roll after tuning*

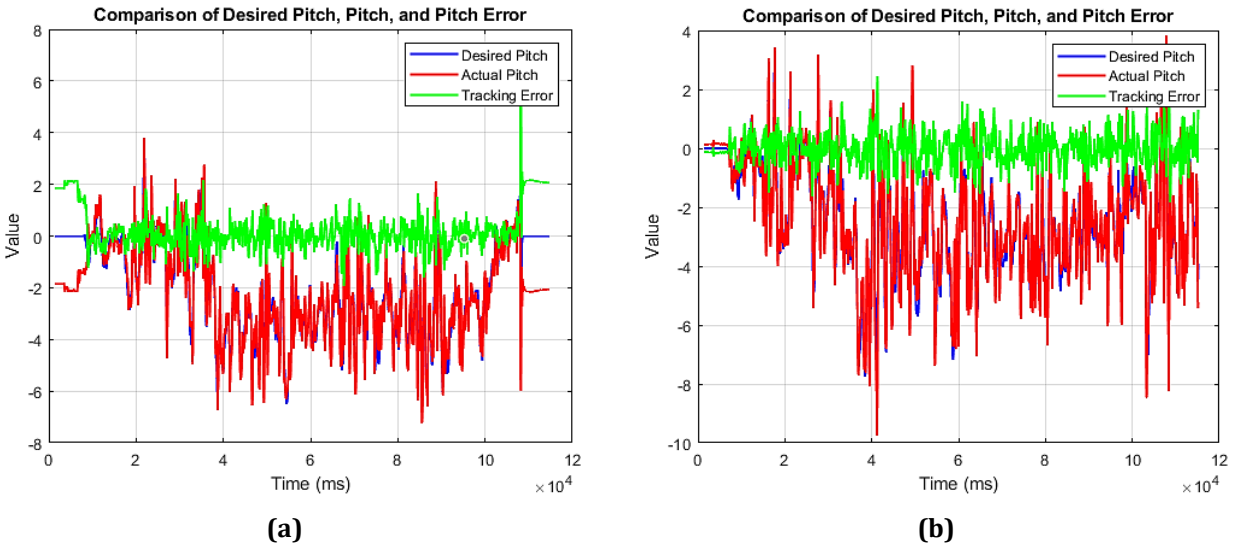

Fig. 12 *(a) Pitch vs desired pitch before tuning & (b) Pitch vs desired pitch after tuning*

Fig. 12 show the green line tends to close the gap near to red and blue lines. It is due to the average error pitch before and after tuning is 0.257574 and 0.01298 respectively. Similarly, for pitch, the average error decreased by 87.8%, with P and I value adjusted from 0.135 to 0.062. This resulted in reduced oscillations and better alignment between the desired and actual pitch values, improving stability when the drone is counteracting the lateral force from the pressurized hose.

5. Conclusion

The TiungLap drone, developed by UTHM, is designed to safely and efficiently clean high-rise building windows. Traditional window-cleaning methods are risky and slow, especially for skyscrapers. TiungLap solves this by using a tethered system that provides continuous water or cleaning solutions, allowing the drone to stay lightweight and operate for longer periods. The drone's advanced features, like real-time monitoring, precise GPS navigation, and obstacle detection, help it clean buildings accurately and safely. TiungLap is specifically designed to clean large glass surfaces on tall buildings, making it more effective than smaller cleaning robots typically used for homes. By using TiungLap, the need for human workers in dangerous conditions is reduced, and the cleaning process becomes faster and more efficient, offering a modern solution for maintaining skyscrapers.

The TiungLap drone was developed to address the specific challenges associated with cleaning high-rise building windows, particularly focusing on safety, operational efficiency, and cleaning precision. The objective of optimizing thrust power consumption and control stability during cleaning operations was successfully achieved through several key advancements. The quadcopter system, utilizing four X9 motors, demonstrated a maximum thrust of 21.23 kgf per motor, ensuring it could lift the 22 kg payload effectively. Additionally, the power analysis revealed an overall system power consumption of 7421.25W, which allowed for consistent and sustained operation during cleaning tasks. The drone's stability was a significant challenge due to the external forces from the tethered hose. However, through manual tuning of the PID controller, the roll error was reduced by 94.9% and the pitch error by 87.8%, resulting in significantly improved stability during operation. These performance improvements highlight the drone’s ability to maintain control and precision in challenging environments.

In summary, TiungLap meets the initial objectives by offering a reliable, efficient, and safer alternative for high-rise window cleaning. While its performance in thrust and stability optimization is promising, further enhancements, such as extending flight endurance and refining control algorithms for managing external forces, remain essential for future iterations. Future research could focus on improving the drone’s stability when handling external forces, like the pressure from the tethered cleaning system. Additionally, refining its power supply for longer operational times and enhancing its obstacle detection capabilities can make it even more reliable in complex environments. Exploring lighter materials or more efficient propulsion systems could also help reduce energy consumption, making the drone more effective for larger-scale operations. Addressing these areas will push TiungLap closer to becoming a widely adopted, fully autonomous cleaning solution for high-rise buildings

Acknowledgement

This research was supported by Universiti Tun Hussein Onn Malaysia (UTHM) through the UTHM Contract Grant (vot Q540) and Product Development Grant (vot B106).

Conflict of Interest

Authors declare that there is no conflict of interest regarding the publication of the paper.

Author Contribution

The authors have no disclosure conflict of interest to declare and are satisfied with their own contribution to the whole project and writings. Ahmad Fathan Fadzulli tackle in Conceptualization, Methodology, Investigation, Data Curation, Formal Analysis, Validation, Writing - Original Draft Preparation, Visualization. As the lead author, Fathan was responsible for the design and execution of the experiments, data collection and tabulation, performance analysis, and the initial writing and formatting of the manuscript.

Omar Mohd Faizan Marwah is the Supervision, Project Administration, Funding Acquisition, Conceptualization, Methodology, Writing - Review & Editing. Dr. Omar, as the main supervisor, provided the overall research direction, secured the necessary funding, and was instrumental in reviewing and critically revising the manuscript for intellectual content.

Mohammad Zulafif Rahim is in Supervision, Resources, Methodology, Writing - Review & Editing. Dr. Zulafif co-supervised the research, provided technical guidance on the methodology, and contributed to the review and editing of the manuscript. Siti Juita Mastura Salleh, Zamri Omar, Suhaimi Hassan, Reazul Haq Abdul Haq: Resources, Writing - Review & Editing. The co-authors provided valuable resources, technical insights, and contributed to the final review and editing of the manuscript. These co-authors contribute to suggesting the data is tabulated using the ScorpionCalc.

References

[1] T. W. Seo, Y. Jeon, C. Park, and J. Kim, "Survey on Glass And Façade-Cleaning Robots: Climbing Mechanisms, Cleaning Methods, and Applications," Apr. 01, 2019, *Korean Society for Precision Engineering*. https://doi.org/10.1007/s40684-019-00079-4.

[2] Z. Li, Q. Xu, and L. M. Tam, "A survey on techniques and applications of window-cleaning robots," *IEEE Access*, vol. 9, pp. 111518–111532, 2021, https://doi.org/10.1109/ACCESS.2021.3103757.

[3] Kuala Lumpur City, "Merdeka 118, the World's Second Tallest Building." Accessed: Jul. 01, 2024. [Online]. Available: https://kualalumpurcity.my/merdeka-118-kuala-lumpur-skyscraper/

[4] Nikolaos Baras, Georgios Nantzios, Dimitris Ziouzios, and Minas Dasygenis, *Autonomous Obstacle Avoidance Vehicle Using LIDAR and an Embedded System*. IEEE, 2019 https://doi.org/10.1109/MOCAST.2019.8742065.

[5] U. G. Sefercik and M. Nazar, "Consistency Analysis of RTK and Non-RTK UAV DSMs in Vegetated Areas," *IEEE J Sel Top Appl Earth Obs Remote Sens*, vol. 16, pp. 5759–5768, 2023, https://doi.org/10.1109/JSTARS.2023.3288947.

[6] RCDrone, "Hobbywing X9 Power System - 9616 110KV 12-14S with ESC+Propeller+Motor ComBo for 10L16L/22L multirotor Agriculture Drone." Accessed: Aug. 20, 2024. [Online]. Available: https://rcdrone.top/products/hobbywing-x9-power-system?currency=USD&variant=43856626385120&utm_source=google&utm_medium=cpc&utm_campaign=Google%20Shopping&stkn=677f40c1dee9&gad_source=4&gclid=Cj0KCQjw2ou2BhCCARIsANAwM2GmtA9YhHxBlOrDsv-urIHDKX8jCUv-ewIJrVSrF7zeAOle3VbvX0QaAh3lEALw_wcB

[7] C. Gangu Naidu *et al.*, "A Concise Review on Carbon Fiber-Reinforced Polymer (CFRP) and Their Mechanical Significance Including Industrial Applications," 2023. [Online]. Available: www.intechopen.com

[8] Nurul Farhana Roszaini and S. A. Othman, "The Investigation of General Properties of Carbon Fiber (CF) Composites - Preliminary Study," *Journal of Applied Science & Process Engineering*, vol. 10, no. 1, pp. 59–65, Apr. 2023, https://doi.org/10.33736/jaspe.5528.2023.

[9] L. M. Alhadad, H. R. Akhmad, A. Novel, M. D. S. Widyatmaja, J. Sembiring, and K. Ben Loda, "Wearable Universal Long-Range Hand-Gestured UAV Radio Control," in *2023 IEEE International Conference on Aerospace Electronics and Remote Sensing Technology, ICARES 2023*, Institute of Electrical and Electronics Engineers Inc., 2023. https://doi.org/10.1109/ICARES60489.2023.10329800.

[10] D. A. Yusuf *et al.*, "A Review of Conceptual Design and Self Health Monitoring Program in a Vertical City: A Case of Burj Khalifa, U.A.E.," Apr. 01, 2023, *MDPI*. https://doi.org/10.3390/buildings13041049.

[11] A. Khodabandeh, "Single-station PPP-RTK: correction latency and ambiguity resolution performance," *J Geod*, vol. 95, no. 4, Apr. 2021, https://doi.org/10.1007/s00190-021-01490-z.

[12] E. Maheswari, V. Balaji, G. Ezhilarasi, D. Lakshmi, A. Abirami, and M. Soundarya, "LIDAR Micro Drone with Proximity Sensing," in *2023 Intelligent Computing and Control for Engineering and Business Systems, ICCEBS 2023*, Institute of Electrical and Electronics Engineers Inc., 2023. https://doi.org/10.1109/ICCEBS58601.2023.10449313.

[13] Robu.In, "SLAMTEC Slamtec RPLiDAR A2M12 360 Degree Laser Scanner Kit – 12M Range." Accessed: Aug. 15, 2024. [Online]. Available: https://robu.in/product/slamtec-rplidar-a2m12-360-degree-laser-scanner-kit-12m-range/

[14] `Abdul Aziz Ahmad Kamal, M. A. Ahmad, M. J. Ahmad, and M. Srivanit, "3D Model of Tunku Tun Aminah Library Using Unmanned Aerial Vehicle (UAV)," *International Journal of Sustainable Construction Engineering and Technology*, vol. 14, no. 5, pp. 408–415, 2023, https://doi.org/10.30880/ijscet.2023.14.05.034.

[15] L. Ding, M. Kerber, C. Kunisch, and B. J. P. Kaus, "Plastic yielding of glass in high-pressure torsion apparatus," *Int J Appl Glass Sci*, vol. 10, no. 1, pp. 17–26, Jan. 2019, https://doi.org/10.1111/ijag.12847.

[16] C. Liu, R. Wang, W. Wang, X. Hu, W. Wu, and F. Liu, "Different Irrigation Pressure and Filter on Emitter Clogging in Drip Phosphate Fertigation Systems," *Water (Switzerland)*, vol. 14, no. 6, Mar. 2022, https://doi.org/10.3390/w14060853.

[17] M. Muchlas Sony and Y. Suhandini, "Implementasi Hi-Pressure Fog Spray Dust Suppression System Di PLTU Paiton 9," vol. 8, 2018, https://doi.org/10.20961/mekanika.v20i1.48208.

[18] D. T. Yusupov, M. Rakhmatova, and S. Tashmatova, "Study of optimal temperature during adsorption cleaning of transformer oil under conditions of long-term operation," in *E3S Web of Conferences*, EDP Sciences, Apr. 2023. https://doi.org/10.1051/e3sconf/202338304058.

[19] J. Ho Lee, W. Seok Moon, and S. Bin Park, "Numerical Simulation Of Thermophoretic Particle Decontamination In Clean Rooms," 1996. doi: https://doi.org/10.1007/BF02705882.

[20] RCDrone, "Herewin RC LiPo Battery 6S 22.2V 22000mAh 20C For RC Car Airplane Tank Drone Toy Models 6s RC Agriculture Drone Battery," 2024. Accessed: Aug. 20, 2024. [Online]. Available: https://rcdrone.top/products/herewin-rc-lipo-battery-6s-22-2v-22000mah-20c?currency=USD&variant=44123367047392&utm_source=google&utm_medium=cpc&utm_campaign=Google%20Shopping&stkn=677f40c1dee9&gad_source=1&gclid=Cj0KCQjw2ou2BhCCARIsANAwM2GS-FNuALmKMOr3dIOs6GM6mSbXS8bdrxCUgZK7reE4Lv4EAniiVvMaAqLyEALw_wcB

[21] Y. Zhang, J. Xu, S. Yang, C. Deng, F. Chen, and F. Lei, "Battery module capacity fade model based on cell voltage inconsistency and probability distribution," *Advances in Mechanical Engineering*, vol. 9, no. 9, pp. 1–13, Sep. 2017, https://doi.org/10.1177/1687814017730757.

[22] H. G. Jorge, L. M. G. de Santos, N. F. Álvarez, J. M. Sánchez, and F. N. Medina, "Operational study of drone spraying application for the disinfection of surfaces against the COVID-19 pandemic," *Drones*, vol. 5, no. 1, 2021, https://doi.org/10.3390/drones5010018.

[23] V. Gomez, N. Gomez, J. Rodas, E. Paiva, M. Saad, and R. Gregor, "Pareto optimal PID tuning for Px4-based unmanned aerial vehicles by using a multi-objective particle swarm optimization algorithm," *Aerospace*, vol. 7, no. 6, Jun. 2020, https://doi.org/10.3390/AEROSPACE7060071.

[24] B. Hament and P. Oh, "A Pressure Washing Hosing-Drone - Mitigating Reaction Forces and Torques," in *2022 International Conference on Unmanned Aircraft Systems, ICUAS 2022*, Institute of Electrical and Electronics Engineers Inc., 2022, pp. 468–477. https://doi.org/10.1109/ICUAS54217.2022.9836101.

[25] J. T. Zou and X. Y. Dai, "The Development of a Visual Tracking System for a Drone to Follow an Omnidirectional Mobile Robot," *Drones*, vol. 6, no. 5, May 2022, https://doi.org/10.3390/drones6050113.

[26] Hobbywing, "XRotor X9 - 好盈科技." Accessed: Sep. 04, 2024. [Online]. Available: https://www.hobbywing.com/en/products/xrotor-x9109.html

[27] S. M. Lee, W. H. Ng, J. Liu, S. K. Wong, S. Srigrarom, and S. Foong, "Flow-Induced Force Modeling and Active Compensation for a Fluid-Tethered Multirotor Aerial Craft during Pressurised Jetting," *Drones*, vol. 6, no. 4, Apr. 2022, https://doi.org/10.3390/drones6040088.

[28] Shawndy Michael Lee *et al.*, *Hybrid Kinematics Modelling for an Aerial Robot with Visual Controllable Fluid Ejection*. IEEE, 2020. https://doi.org/10.1109/AIM43001.2020.9158941.